Since January 2020 Elsevier has created a COVID-19 resource centre with free information in English and Mandarin on the novel coronavirus COVID-19. The COVID-19 resource centre is hosted on Elsevier Connect, the company's public news and information website.

Elsevier hereby grants permission to make all its COVID-19-related research that is available on the COVID-19 resource centre - including this research content - immediately available in PubMed Central and other publicly funded repositories, such as the WHO COVID database with rights for unrestricted research re-use and analyses in any form or by any means with acknowledgement of the original source. These permissions are granted for free by Elsevier for as long as the COVID-19 resource centre remains active.

Food Microbiology 76 (2018) 346–353

Contents lists available at ScienceDirect

Food Microbiology

journal homepage: www.elsevier.com/locate/fm

# Monomeric catechin and dimeric procyanidin B2 against human norovirus surrogates and their physicochemical interactions

Dan Liu[a,1], Jianjun Deng[b,1], Snehal Joshi[c], Pengbo Liu[d], Chao Zhang[a], Yan Yu[a], Ruijuan Zhang[a], Daidi Fan[b], Haixia Yang[a,**], Doris H. D'Souza[c,*]

[a] Nutrition and Food Safety Department, College of Public Health, Health Science Center, Xi'an Jiaotong University, Xi'an, 710061, China
[b] Shaanxi Key Laboratory of Degradable Biomedical Materials, College of Chemical Engineering, Northwest University, Xi'an, 710069, China
[c] Department of Food Science, The University of Tennessee, Knoxville, TN, USA
[d] Rollins School of Public Health, Emory University, Atlanta, GA, 30322, USA

ARTICLE INFO

*Keywords:*
Procyanidin B2
Norovirus
P domain
Interaction

ABSTRACT

Plant polyphenols have shown antiviral activity against several human pathogens, but their physicochemical interactions are not well-understood. The objectives of this study were to compare the antiviral activity between monomeric catechin and dimeric procyanidin B2 (PB2) using cultivable human norovirus surrogates (feline calicivirus (FCV-F9) and murine norovirus (MNV-1)) and to understand their potential antiviral mechanism using virus-like particles (VLPs) and the P domain of human norovirus GII (HNoV GII.4). Surrogate viruses at 5 log PFU/mL were treated with 0.5–5 mg/mL monomeric catechin monohydrate, PB2 or phosphate buffered saline (PBS, pH 7.2; control) at 37 °C over 24 h. Infectivity was determined using plaque assays and data from triplicate experiments were statistically analyzed. PB2 at 0.5 mg/mL and 1 mg/mL reduced FCV-F9 to undetectable levels after 3 h and MNV-1 by 0.21 and 1.23 log PFU after 24 h, respectively. Monomeric catechins at 1 mg/mL reduced FCV-F9 to undetectable levels after 6 h and MNV-1 titers to undetectable levels after 24 h. In addition, PB2 was shown to directly bind the P domain, the main capsid structure of HNoVs in the ratio of 1:1 through spontaneous interactions. Electrostatic interactions played a dominant role between PB2 and the P domain. PB2 significantly altered tertiary but not secondary structures of VLPs. Transmission electron microscopy demonstrated that PB2 aggregated VLPs, further indicating interactions between them. These findings indicate that PB2 causes structural changes of the P domain of VLPs, mainly through direct interaction leading to HNoV inactivation.

## 1. Introduction

Human noroviruses (HNoVs) of the *Caliciviridae* family are recognized as the leading causes of acute gastroenteritis outbreaks and sporadic gastroenteritis in both developed and developing countries, with newly emergent strains that are recognized as being increasingly virulent particularly to the immunocompromised patients (Su and D'Souza, 2012; Zhang et al., 2012; Kageyama et al., 2004). In the United States, the CaliciNet reported that HNoVs accounted for 80–95% of all cases of gastroenteritis outbreaks from 2009 to 2013 (Hall et al., 2013; Vega et al., 2014). Moreover, studies on the prevalence of HNoV infections in China were also widely described in recent years (Mai et al., 2013; Xue et al., 2013). The HNoV genotype GII.4 that caused more than 85% of all outbreaks was reported to be the most prevalent and infectious strain in past years (Vega et al., 2014; Zheng et al., 2010). HNoVs are still difficult and laborious to cultivate (albeit at low infectious titers currently) (Ettayebi et al., 2016). The expression of the capsid protein in a baculovirus expression system has shown to result in the self-assembly of virus-like particles (VLPs) that are morphologically and antigenically similar to the native infectious virion (Jiang et al., 1992). VLPs are used to determine antiviral activity along with cultivable surrogates such as feline calicivirus (FCV-F9), murine norovirus (MNV-1) and Tulane virus (Jiang et al., 1992; Joshi et al., 2017; Su and D'Souza, 2011, 2013; Su et al., 2010a,b,c). The X-ray crystal structure of the prototype human norovirus VLPs identified two major domains, the shell (S) and protruding (P) domains, linked by a hinge of 8 amino acids (Jiang et al., 1992), with the P domain further divided into P1 and P2 subdomains. The P2 domain is evolutionarily highly variable and

* Corresponding author.
** Corresponding author.
*E-mail addresses:* yanghx@xjtu.edu.cn (H. Yang), ddsouza@utk.edu (D.H. D'Souza).
[1] Dan Liu and Jianjun Deng contributed equally to this work.

https://doi.org/10.1016/j.fm.2018.06.009
Received 21 January 2018; Received in revised form 15 May 2018; Accepted 15 June 2018
Available online 21 June 2018
0740-0020/ © 2018 Published by Elsevier Ltd.

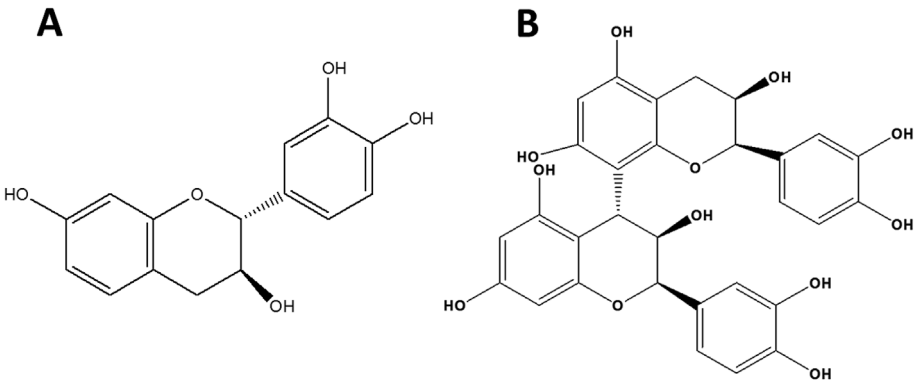


**Fig. 1.** Comparison of the chemical structures of Catechin (A) and PB2 (B).

responsible for binding to human histo-blood group antigens (HBGAs) as ligands or host receptors for attachment, in an early infection event that most likely controls host susceptibility and resistance to HNoVs (Tan et al., 2004; Tan and Jiang, 2011). Any substance or compounds that can block HNoV–HBGA interaction is likely to inhibit HNoV host entry, infection and thus function as suitable candidate antivirals against HNoVs (Jiang et al., 2004).

Procyanidins, the oligomeric forms of flavan-3-ols, are polyphenol compounds from the flavonoid group which constitute oligomers or polymers of (+)-catechin and/or (−)-epicatechin units (Fig. 1A), linked mainly through C4-C8 or C4-C6 bonds (Howell et al., 1998, 2005). These procyanidins are found in a wide variety of food commodities including vegetables and fruits, such as grapes, berries, apples, litchi, tea, cereals, and cocoa beans (Hammerstone et al., 2000; Zhang et al., 2012), with each having varying composition and percentage of monomeric catechins, epicatechin, oligomers and polymers. The most ubiquitous procyanidin dimers present in nature and human diets are the B-type procyanidins, with units that are linked via C4-C8 bonds (Fig. 1B) (Lizarraga et al., 2007; Joshi et al., 2017). These substances are known to exhibit an array of health benefits and pharmacological effects such as anti-inflammatory, antimicrobial and antioxidant activities (Alvarez et al., 2012; Khurana et al., 2013; Terra et al., 2009; Yang et al., 2014a). As reported earlier, these polyphenols have shown antiviral activity against influenza virus (Yang et al., 2014b), hepatitis C virus (Takeshita et al., 2009) and severe acute respiratory syndrome coronavirus (Zhuang et al., 2009). Previous studies suggest that antiviral activity is associated with oligomeric procyanidins. For example, oligomeric procyanidins inhibit herpes simplex virus type-1 (HSV-1) by abolishing virus entry into the host cell caused by blocking attachment to the cell surface (Gescher et al., 2011; Kimmel et al., 2011). The procyanidin B2, A2 and especially C1 showed anti-HIV activity *in vitro* (Shahat et al., 1998). Additionally, Su and D'Souza (2011, 2013) reported that grape seed extract, which contains large quantities of monomeric, dimeric and trimeric procyanidins, and also cranberry proanthocyanidins (C-PAC) exhibited antiviral activity against the HNoV cultivable surrogates, FCV-F9 and MNV-1 (Su and D'Souza, 2011, 2013; Su et al., 2010a,b). More recently, blueberry procyanidins were reported to have antiviral effects against HNoV surrogates (Joshi et al., 2016, 2017). However, the specific potential mechanisms of antiviral activities of the various plant polyphenols are still not well-understood.

The objectives of this study were to determine the antiviral effects of monomeric catechin and procyanidin B2 (PB2) against HNoVs using cultivable HNoV surrogates, FCV-F9 and MNV-1. Another objective was to determine the interaction between PB2 and the HNoV capsid protein VLPs or P domain peptide using spectral techniques and transmission electron microscopy (TEM). This study provided evidence that PB2 (dimeric catechins) can directly bind to the capsid of HNoVs and can serve as a potential candidate antiviral therapeutic option.

## 2. Materials and methods

### 2.1. Viruses and cell lines

FCV-F9 and Crandell Reese Feline Kidney (CRFK) host cells were obtained from ATCC (Manassas, VA) as reported in our earlier studies (Joshi et al., 2017). Similarly as reported earlier, MNV-1 was kindly provided by Dr. Skip Virgin (Washington Univ., St. Louis, MO) and its RAW 264.7 host cells were obtained from the University of Tennessee-Knoxville and propagated and maintained as before (Joshi et al., 2017; Su et al., 2010a,b). Briefly, both viral host cell lines were maintained using Dulbecco's Modified Eagle's Medium/Ham's F-12 (DMEM-F12; HyClone Laboratories, Logan, UT) containing 10% heat-inactivated fetal bovine serum (FBS, HyClone Laboratories) and Antibiotic-Antimycotic (Thermo Fisher Scientific) at 37 °C in an incubator with 5% $CO_2$ as reported earlier (Su et al., 2010a,b,c).

### 2.2. Comparison of antiviral activity of monomeric and dimeric procyanidins

Antiviral activity of catechin hydrate (Sigma Aldrich, USA) and PB2 (Sigma Aldrich) against FCV-F9 and MNV-1 was determined and compared using methods described in earlier studies (Joshi et al., 2016; Su et al., 2010a,b,c). Briefly, equal amounts of each virus at 5 log PFU/mL were mixed with equal amounts of catechin hydrate (to 1 or 5 mg/mL final concentration) or PB2 (0.5 or 1 mg/mL final concentration) (both were in powder form and were dissolved solution containing 10% ethanol and 90% distilled deionized water, with a pH around 5) or phosphate buffered saline (PBS, pH 7.2) for 3, 6, and 24 h at 37 °C. Reactions were stopped in DMEM-F12 containing 10% FBS and serially diluted ten-fold in DMEM-F12 containing 2% FBS. Viral infectivity was evaluated using standardized plaque assays in six-well plates containing confluent host cells in duplicate for each replicate treatment as described before (Fino and Kniel, 2008; Su et al., 2010b).

### 2.3. Effect of catechin hydrate and PB2 on host cells lines

Cytopathic effects of catechin hydrate and PB2 treatments on the host cell lines were also determined. The maximum concentration of catechin hydrate used in the viral treatment and assays was 10 mg/mL and for PB2 was 1 mg/mL, however, the host cell lines were only exposed to a maximum 20-fold dilution of the treatment after stopping of the treatment. Thus, each individual host cell line was exposed to catechin hydrate at 0.5 mg/mL or PB2 at 0.05 mg/mL for 2–24 h at 37 °C and observed under the optical microscope to determine visible changes in cell morphology or cytopathic effects.

**Table 1**
Effect of monomeric catechins and procyanidin B2 on FCV-F9 titers at 37 °C over 24 h (Recovered titers in Log PFU/mL).

| Time | PBS (pH 7.2) | Catechin hydrate | | PB2 | |
|---|---|---|---|---|---|
| (h) | | 5 mg/mL | 1 mg/mL | 1 mg/mL | 0.5 mg/mL |
| 1 | 4.71 ± 0.18$^{A}$ | 0$^{C}$ | 4.73 ± 0.37$^{A}$ | 4.04 ± 0.24 $^{AB}$ | 4.45 ± 0.05$^{A}$ |
| 3 | 4.71 ± 0.15$^{A}$ | 0$^{C}$ | 3.97 ± 0.16$^{B}$ | 0$^{C}$ | 0$^{C}$ |
| 6 | 4.77 ± 0.01$^{A}$ | 0$^{C}$ | 0$^{C}$ | 0$^{C}$ | 0$^{C}$ |
| 24 | 4.73 ± 0.04$^{A}$ | 0$^{C}$ | 0$^{C}$ | 0$^{C}$ | 0$^{C}$ |

$^{A, B, C,}$ Different letters denote significant differences when compared between columns ($p < 0.05$). Detection limit for the assay was 2 log PFU/mL.

### 2.4. Characterization of the VLPs bound to PB2

HNoV GII.4 VLPs were expressed in the commercially available baculovirus expression system (Invitrogen, Carlsbad, CA) at Emory University. The procedures followed were described earlier in detail for the polymerase chain reaction (PCR) amplification, cloning, transfection, expression, VLP extraction and purification, in a previous study (Liu et al., 2015). After the VLPs were examined and confirmed by electron microscopy and immunoblotting, they were used in the TEM experiments as capsid proteins to determine the effects of binding. TEM data images were collected using a H-7650 electron microscope (Hitachi, Japan) operating at 30 k, after VLP solutions (0.2 μg/μL) were incubated for 1 h with PB2 (0.1 mM) in 10 mM PBS buffer, pH 7.4. These solutions were then concentrated using Microcon ultrafilters (Microcon YM-100) with a 100-kDa cutoff and then standard protocols were followed of transferring to carbon-coated copper grids before visualization.

### 2.5. Fluorescence spectra of HNoV GII.4 P2 domain

Fluorescence spectra were performed (Xi'an Jiaotong University in China) using an RF-5301PC fluorescence spectrophotometer (Shimadzu, Japan) equipped with 1.0 cm quartz cells and a thermostatically controlled water bath. The fluorescence spectra were measured in the range of 300–450 nm at three different reaction temperatures (298, 303, and 310 K) with the excitation wavelength being 280 nm. The concentration of the P domain of the HNoV capsid, expressed in *E. coli* (Tan et al., 2004), provided as a gift from Dr. Tan (Rollins School of Public Health, Emory University), was 8.41 μM in 100 mM NaCl and 10 mM PBS, pH 7.4. The titrations were conducted by adding 2 μL increments of PB2 (4.21 mM) to 1 mL of the P domain solution, and with scanning of fluorescence spectra after each addition.

### 2.6. Ultraviolet–Visible (UV) spectra of HNoV GII.4 P2 domain

UV–VIS spectra were measured using a Cary 50 Bio ultraviolet spectrometer (Varian Palo Alto, USA) with the scanning wavelength from 240 to 400 nm. The concentration of the P domain was 8.41 μM in 100 mM NaCl and 10 mM PBS buffer, pH 7.4, similar to as described above. Also, the titrations were conducted by the addition of 2 μL increments of PB2 (4.21 mM) to 1 mL P domain solution as described above. All the spectra were scanned continuously with three replicates.

### 2.7. Circular dichroism (CD) spectra of HNoV GII.4 P2 domain

CD spectra were recorded with a Chirascan spectropolarimeter (Applied Photophysics, Britain), using a quartz cuvette of 1 mm optical path length. The P domain was dissolved in 0.5 mM PBS buffer, pH 7.4. CD spectra were scanned at the far UV range (190–260 nm) with three replicates at 20 nm/min, bandwidth = 1 nm. The CD data was expressed in terms of mean residual ellipticity ($\theta$) in degrees·cm$^{2}$·dmol$^{-1}$. The induced ellipticity was defined as the ellipticity of the PB2-P domain mixture, minus the ellipticity of PB2 alone at the same conditions. Percentage of secondary structure was calculated using the web-based program K2D (http://www.emblheidelberg.de/~andrade/k2d).

### 2.8. Statistical analysis

Data were expressed as mean ± S.D. from three independent experiments. Student *t*-test and one-way ANOVA followed by Tukey's post hoc test were used for statistical analysis, where $P < 0.05$ was considered significant.

## 3. Results

### 3.1. Comparison of antiviral activity of monomeric and polymeric catechins

Monomeric catechin hydrate at 1 mg/mL was shown to reduce FCV-F9 titers to undetectable levels after 6 h, while increased concentration of 5 mg/mL monomeric catechin hydrate reduced FCV-F9 titers to non-detectable levels within a shorter time of 1 h (Table 1). The dimeric B-type procyanidin, PB2 at lower concentrations of 0.5 and 1 mg/mL was shown to reduce FCV-F9 titers to undetectable levels after 3 h. In comparison, earlier studies showed that blueberry procyanidins (B-PACs, 0.5 mg/mL) and cranberry procyanidins (C-PACs, 1.2 mg/mL) could reduce FCV-F9 titers to undetectable within 1 h at 37 °C (Joshi et al., 2016; Su et al., 2010a,b).

The present study showed that MNV-1 had lower titer reduction with both monomeric catechin and PB2 treatment compared to FCV-F9. Reductions in MNV-1 titers of 0.42 ± 0.09 log PFU/mL and 1.76 ± 0.20 log PFU/mL were obtained after 3 h with 1 mg/mL and 5 mg/mL catechin hydrate, respectively. However, MNV-1 titers were reduced to undetectable levels after 6 h of treatment with 5 mg/mL catechin hydrate and after 24 h of treatment with 1 mg/mL catechin hydrate. Only after 24 h using PB2 at 1 mg/mL could a significant reduction in MNV-1 titers of 1.23 ± 0.11 log PFU/mL be obtained

**Table 2**
Effect of monomeric catechins and procyanidin B2 on MNV-1 titers at 37 °C over 24 h (Recovered titers in Log PFU/mL).

| Time | PBS (pH 7.2) | Catechin hydrate | | PB2 | |
|---|---|---|---|---|---|
| (h) | | 5 mg/mL | 1 mg/mL | 1 mg/mL | 0.5 mg/mL |
| 3 | 4.80 ± 0.07$^{A}$ | 3.04 ± 0.20$^{B}$ | 4.38 ± 0.09$^{A}$ | 4.55 ± 0.16$^{A}$ | 4.65 ± 0.05$^{A}$ |
| 6 | 4.41 ± 0.04$^{A}$ | 0$^{C}$ | 4.63 ± 0.03$^{A}$ | 4.67 ± 0.08$^{A}$ | 4.49 ± 0.08$^{A}$ |
| 24 | 4.64 ± 0.04$^{A}$ | 0$^{C}$ | 0$^{C}$ | 3.41 ± 0.15$^{B}$ | 4.43 ± 0.07$^{A}$ |

$^{A, B, C,}$ Different letters denote significant differences when compared between columns ($p < 0.05$). Detection limit for the assay was 2 log PFU/mL.

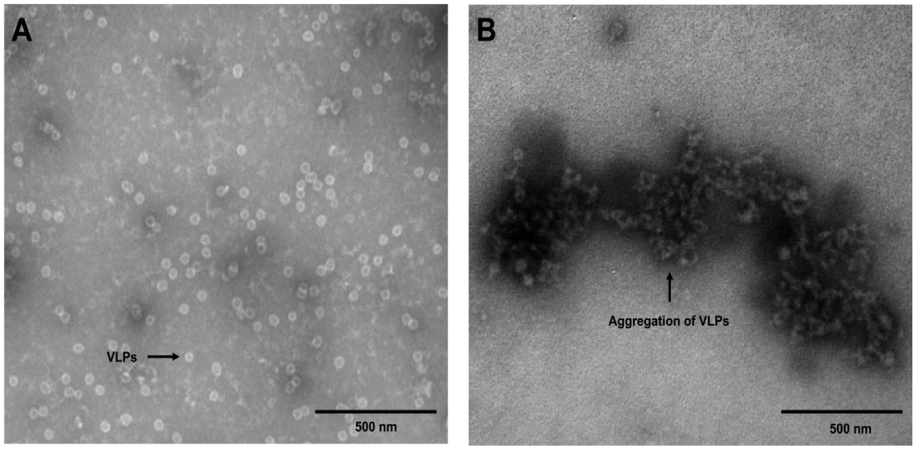


**Fig. 2.** TEM images of VLPs in the absence (A) and presence (B) of PB2 (Conditions for VLPs: [PB2] = 0.1 mM; VLPs, 0.2 μg/μL in 10 mM PBS, pH 7.4, 25 °C; samples were negatively stained by 2% uranyl acetate).

(Table 2). In comparison, B-PAC at 1 mg/mL was shown to reduce MNV-1 titers to undetectable after 3 h of treatment at 37 °C (Joshi et al., 2016), while 0.5 mg/mL C-PAC reduced MNV-1 titers to undetectable after 6 h of treatment at 37 °C (Su et al., 2010b).

### 3.2. Effect of monomeric catechin hydrate and PB2 on host cells lines

During the experiments involving treatment of viruses with monomeric catechins or PB2, the cells are exposed to a maximum of 20-fold dilution of these compounds and the host cells showed no cytopathic effects at 0.5 mg/mL catechin hydrate or 0.05 mg/mL PB2 when visualized under the optical light microscope. This indicated that the effects observed were due to the treatments themselves and not due to any effects on the host cells.

### 3.3. TEM analysis

To further confirm the previously observed results of binding of the polyphenols to the viral particles, the interaction between PB2 and purified recombinant VLPs was also characterized by TEM (Fig. 2). In Fig. 2A, VLPs which have a round shape with a diameter of ~40 nm, dispersed evenly in the PBS buffer system were observed, when PB2 was not added. However, with the addition of PB2, the VLP particles assembled together/aggregated and their size increased (Fig. 2B), indicating that an interaction between PB2 and VLP particles led to the aggregation of capsid proteins.

### 3.4. Binding studies between the viral P domain protein and PB2

Fluorescence spectroscopy is a useful tool to relay some information about the binding of small molecules to proteins, such as the binding mechanism, binding mode, binding constants and binding sites (Brogan et al., 2003; Yang et al., 2014c). The interaction between PB2 and the P domain protein (purity and identity of P domain is depicted by SDS-PAGE in the Supplemental Fig. S1) was evaluated by monitoring the intrinsic fluorescence intensity changes of the P domain upon addition of PB2. The fluorescence spectra of P domain protein in the absence and presence of different concentrations of PB2 in PBS buffer (pH 7.4) are shown in Fig. 3. The P domain exhibited a strong fluorescence peak at 329 nm upon excitation at 280 nm, indicating that most of the observed fluorescence was due to the fluorescent tryptophan (Trp) residues. With the increased concentration levels of PB2, the fluorescence of the P domain was significantly quenched accompanied by a slight red shift of maximum emission wavelength from 327 nm to 332 nm, which may be due to the decreased hydrophobicity in and around Trp. These results suggest that the microenvironment of the P domain changed and an

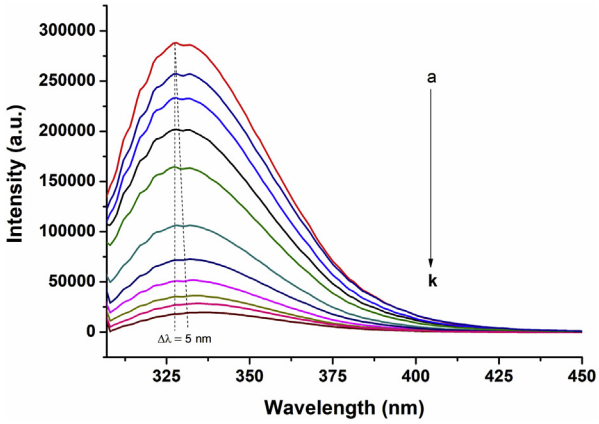


**Fig. 3.** Fluorescence quenching spectra of the P domain peptide at different concentrations of PB2 (a, 0 μM; b, 8.41 μM; c, 16.82 μM; d, 24.23 μM; e, 33.64 μM; f, 42.05 μM; g, 50.46 μM; h, 58.87 μM; i, 67.28 μM; j, 75.69 μM; k, 84.1 μM). The protein sample was excited at 280 nm using a slit-width of 2.5 nm. Emission scans were from 300 nm to 450 nm using a 5 nm slit-width. [P domain] = 8.41 μM, [PBS] = 10 mM, pH 7.4, 25 °C.

interaction between PB2 and the P domain occurs. However, we do recognize the limitation of this binding study, in that besides PB2, other compounds as controls for binding need to be tested which were not carried out in this current study to determine their role in viral inactivation using the Stern-Volmer equation (See supplemental material for more information).

To determine the type of quenching mechanism, the fluorescence data were analyzed by the well-known Stern–Volmer equation (equation S1 in supplemental materials). The curves of $F_0$ (steady state fluorescence intensity in the absence of quencher)/F (steady state fluorescence intensity in the presence of quencher) versus PB2 concentration expressed as [Q] for the interaction between PB2 and P domain are shown in Fig. 4. The perfect linear correlation coefficients can be seen on the plot ($R^2 > 0.99$) when the PB2 concentration is less than $33 \times 10^{-6}$ mol/L, suggesting that the quenching of P domain by PB2 with low concentrations can be interpreted by the Stern–Volmer equation (Fig. 4A). Fig. 4B shows the Stern-Volmer plots of P domain in the presence of PB2 ($5–35 \times 10^{-6}$ mol/L) at three different temperatures (298, 303, and 310 K). Correspondingly, the $K_{SV}$ (Stern–Volmer quenching constant) values at these temperatures are shown in Table 3. All the $K_{SV}$ values for the interaction of P domain with PB2 decreased from $1.87 \times 10^4$ to $1.42 \times 10^4$ L/mol when the temperature increased from 298 to 310 K, indicating a static quenching mechanism. Moreover,

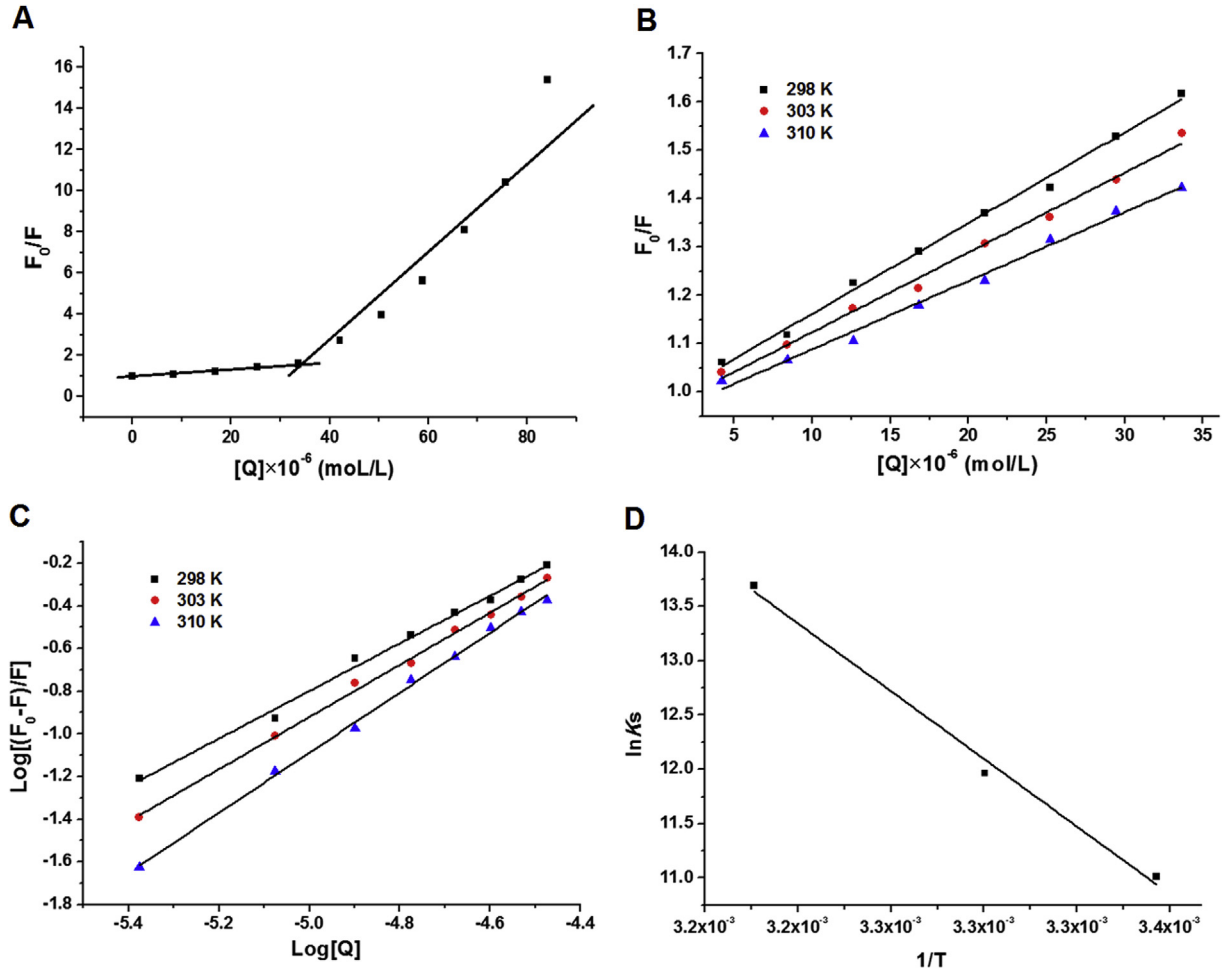


**Fig. 4.** Stern-Volmer curves for the binding of PB2 (A: adding with high concentration 0–80 μM of PB2, B: adding with low concentration 0–35 μM of PB2) with the P domain, double-logarithm plot of the PB2 quenching effect on P domain fluorescence (C), and Van't Hoff plot for the interaction of P domain and B2 (D) at 298, 303, and 310 K. Conditions: [P domain] = 8.41 μM, [PBS] = 10 mM, pH 7.4, [PB2] = 8.41–84.1 μM.

**Table 3**
The quenching constants of the P domain by PB2 at different temperatures.

| pH | T(K) | $K_{SV}$( × $10^4$L·mol$^{-1}$) | $K_q$ ( × $10^{12}$L·mol$^{-1}$·s$^{-1}$) | $R^2$ | S.D. |
|---|---|---|---|---|---|
| 7.4 | 298 | 1.874 | 1.874 | 0.9945 | 0.012 |
| | 303 | 1.651 | 1.651 | 0.9927 | 0.006 |
| | 310 | 1.420 | 1.420 | 0.9916 | 0.010 |

$R^2$ is the correlation coefficient.S.D. is the standard deviation.
Conditions: [P domain] = 8.41 μM, [PBS] = 10 mM, pH 7.4, [PB2] = 8.41–84.1 μM.

all the corresponding $K_q$ (quenching rate constant) values, a specific constant describing bimolecular collisional deactivation of electronic energy, were more than $2.0 \times 10^{10}$ L/(mol·s), which is another indicator of static quenching.

Based on the slope of the double logarithm regression curve of $\log_{10}$ [($F_0$-F)/F] versus $\log_{10}$ [Q] (equation S2 in supplemental materials; Fig. 4C, $R^2 > 0.99$), the corresponding number of binding sites 'n' and apparent binding constant of chemical with protein ($K_a$) were calculated at different temperatures (Table 4). The number of binding sites was approximately equal to 1 for P domain, suggesting that only one PB2 molecule binds to each P domain peptide.

According to the binding constants at three different temperatures (298 K, 303 K, and 310 K), the thermodynamic parameters are calculated using equations S3-S4 (see supplemental materials) and presented in Table 4 and Fig. 4D. The negative ΔG (Gibbs energy change) values indicated that the binding process of PB2 to P domain was spontaneous. For the interaction forces between PB2 and P domain, the negative enthalpy ΔH ($-172.879$ kJ·mol$^{-1}$) and positive entropy ΔS (671.077 J·K$^{-1}$·mol$^{-1}$) values demonstrated that the electrostatic interactions played a dominant role in the interaction between PB2 and the P domain peptide.

### 3.5. UV spectroscopy results

UV spectroscopy inspects the change of secondary and tertiary structures of protein under the addition of physical and chemical factors. The UV spectroscopy of the P domain peptide in the absence and presence of different concentrations of PB2 in 10 mM PBS (pH 7.4) are shown in Fig. 5A. The maximum absorption peak was observed at 280 nm, indicating that the hydrophobicity of the microenvironment of the P domain decreased. With increasing concentration of PB2, the maximum absorption intensity of the P domain increased significantly, suggesting that the interaction between them leads to the loosening and unfolding of the protein backbone.

### 3.6. CD spectroscopy results

CD spectroscopy was performed in the far-UV region in order to obtain more information about the secondary structure changes of the P domain in the presence of PB2. Fig. 5B shows the CD spectra of the free P domain and bound P domain-PB2 complex. Both of these two spectra

**Table 4**
The binding constant, $K_a$, the number of binding sites, n, and the thermodynamic parameters for the association of PB2 with the P domain.

| pH | T(K) | $K_a$ ($\times 10^5$ L·mol$^{-1}$) | n | $R^2$ | Δ H (kJ·mol$^{-1}$) | ΔG (kJ·mol$^{-1}$) | ΔS (J·mol$^{-1}$ K$^{-1}$) |
|---|---|---|---|---|---|---|---|
| 7.4 | 298 | 0.6053 | 1.116 | 0.9938 | −172.879 | −372.859 | 671.077 |
| | 303 | 1.5704 | 1.223 | 0.9971 | | −376.215 | |
| | 310 | 8.8712 | 1.407 | 0.9974 | | −380.913 | |

$R^2$ is the correlation coefficient.
Conditions: [P domain] = 8.41 μM, [PBS] = 10 mM, pH 7.4, [PB2] = 8.41–84.1 μM.

exhibited negative absorption bands at 208 nm and a weak positive peak at 230 nm and had no significant difference between them. The percentage of secondary structure was also calculated and is shown in Fig. 5C. The P domain contains about 12.1% α-helix, 16.9% β-sheet, 21.3% antiparallel, 21.9% parallel and 55.8% random coil, whereas the addition of PB2 did not change the secondary structure of the P domain peptide.

## 4. Discussion

There are an increasing number of studies reported in literature that determine the antiviral properties of natural polyphenols, and some have also been summarized in literature reviews (D'Souza et al., 2016; D'Souza, 2014; Joshi et al., 2016; Su et al., 2010a,b,c). Once identified, methods for optimizing their delivery and maintaining potency and stability as well as determination of their mode of action are required. One of the reasons that the mechanisms of action are not well understood is because appropriate animal models are currently unavailable. Therefore, this study was undertaken to compare the effects of monomeric catechin hydrate and PB2 against human norovirus surrogates, FCV-F9 and MNV-1. Procyanidins, which are oligomers or polymers of catechin, have been shown to exert a range of bioactivities, such as antioxidation, anti-inflammation as well as antimicrobial effects (Alvarez et al., 2012; Terra et al., 2009; Joshi et al., 2016, 2017). Overall, the polymeric procyanidins showed higher antiviral effects when compared to monomeric catechins (Joshi et al., 2016). Specifically, based on previous literature, procyanidins isolated from both blueberries (B-PAC) and cranberries (C-PAC) were shown to have higher effects against human norovirus surrogates (FCV-F9 and MNV-1) within shorter time and at a lower concentration compared to the commercial PB2 and monomeric catechin. While FCV-F9 titers were earlier reported to be reduced to non-detectable levels with 1 and 2 mg/mL B-PAC after 5 min (Joshi et al., 2016), an increased concentration of 5 mg/mL catechin hydrate was required to reduce FCV-F9 to non-detectable levels with a longer treatment time of 3 h. Also, the lower concentration of monomeric catechin hydrate at 1 mg/mL was found to reduce FCV-F9 to undetectable levels after 6 h in the current study. The dimeric B-type procyanidins, PB2 showed an intermediate activity between that of polymeric procyanidins and monomeric catechin, where 0.5 mg/mL and 1 mg/mL could reduce FCV-F9 to undetectable levels after 3 h. Thus, for FCV-F9, it appears that the antiviral activity follows the order of procyanidin extract (polymeric polyphenols) being greater than PB2, and PB2 being greater than monomeric catechin hydrate.

Earlier work showed that MNV-1 titers were reduced to non-detectable levels with all three concentrations of 1, 2 and 5 mg/mL B-PAC (procyanidins) after 3 h, while this similar reduction occurred only after 6 h with commercially available blueberry juice (Joshi et al., 2016). The current study showed that reductions of 0.42 ± 0.02 and 1.76 ± 0.13 log PFU/mL after 3 h with 1 mg/mL and 5 mg/mL catechin hydrate, respectively, were obtained for MNV-1, while increasing treatment time of 6 h was required to cause reduction of MNV-1 titers to non-detectable levels with 5 mg/mL catechin hydrate. Though, 1 mg/mL PB2 could reduce MNV-1 titers by 1.23 ± 0.11 log PFU/mL only after 24 h. Thus, for MNV-1, the antiviral activity of procyanidins was greater than catechin monohydrate, and monomeric catechin hydrate appeared to have better activity than the dimeric PB2. The difference in responses to the monomeric and dimeric catechins between FCV-F9 and MNV-1 could be speculated to be associated with their varying capsid structure and pH stability.

In earlier studies, when FCV-F9 and MNV-1 at 5 log PFU/mL were mixed with equal volumes of cranberry juice (CJ) or A-type C-PAC at 0.30, 0.60 and 1.20 mg/mL for 1 h at room temperature, FCV-F9 was reported to be reduced to non-detectable levels (Su et al., 2010a,b). While MNV-1 was reported to be reduced by 2.06 log PFU/mL with CJ, and by 2.63, 2.75 and 2.95 log PFU/mL with 0.15, 0.30 and 0.60 mg/mL C-PAC, respectively, after 1 h at room temperature. Thus, it appears that both A-type and B-type procyanidins exhibit antiviral activity against the tested HNoV surrogates. However, these earlier studies showed that a lower concentration of A-type procyanidins from cranberries at 0.3 mg/mL and even at ambient temperature can have similar effects as 0.5 mg/mL B-type procyanidins from blueberries at 37 °C. This current study provides insights on the activity of the molecular structures of polyphenols and should prove beneficial in the design of appropriate preventive anti-viral therapies from natural sources.

A similar trend in titer reduction was observed in the host binding/attachment assays reported earlier for both FCV-F9 and MNV-1 (Joshi et al., 2016). This previous study showed that pre-treatment of host cells with B-type procyanidins had some effect in blocking binding of the virus to the host and thus caused reduction in infectious titers. Therefore, it can be postulated that treatment with B-type procyanidins can exert antiviral activity by destroying the viral capsid structure and blocking the binding receptors, both leading to prevention of host attachment (Joshi et al., 2016).

To understand the broad spectrum and application of these polyphenols from natural sources and particularly cranberries and blueberries for improved function and to improve human health, their effects in model food systems and under gastric conditions along with feeding studies and clinical trials with correlation to food and diet intake need to be undertaken before recommendations can be made as reported earlier (Joshi et al., 2016; Su et al., 2010b). Recently, the effects of B-PAC in model foods and simulated gastric conditions against cultivable HNoV surrogates were also reported (Joshi et al., 2017). Polyphenolic compounds are known to bind to various proteins with different binding affinities leading to changes in the structural and functional properties of both polyphenols and proteins (Soares et al., 2007), which depends on the polyphenol structure, the proteins, and the system conditions. PB2 can bind to proteins, such as bovine serum albumin (BSA) and human salivary α-amylase (Bartolome et al., 2000; Soares et al., 2007). In this study the P domain peptide, which is responsible for binding of the HNoV capsid with HBGAs as ligands or receptors for attachment was used to determine whether PB2 affects the structures of the P domain peptide leading to change of the activity. The interaction between PB2 and the P domain was determined by using spectroscopy techniques *in vitro*. Fluorescence quenching studies showed that PB2 spontaneously binds to the P domain in the ratio of 1:1 with $K_{SV}$ values from $1.87 \times 10^4$ to $1.42 \times 10^4$ L/mol with the main interaction force being electrostatic interactions. UV and CD spectroscopy showed that PB2 dramatically affected the tertiary structures but did not affect the secondary structures of the P domain. All of these results indicate that a direct interaction between the P domain and PB2

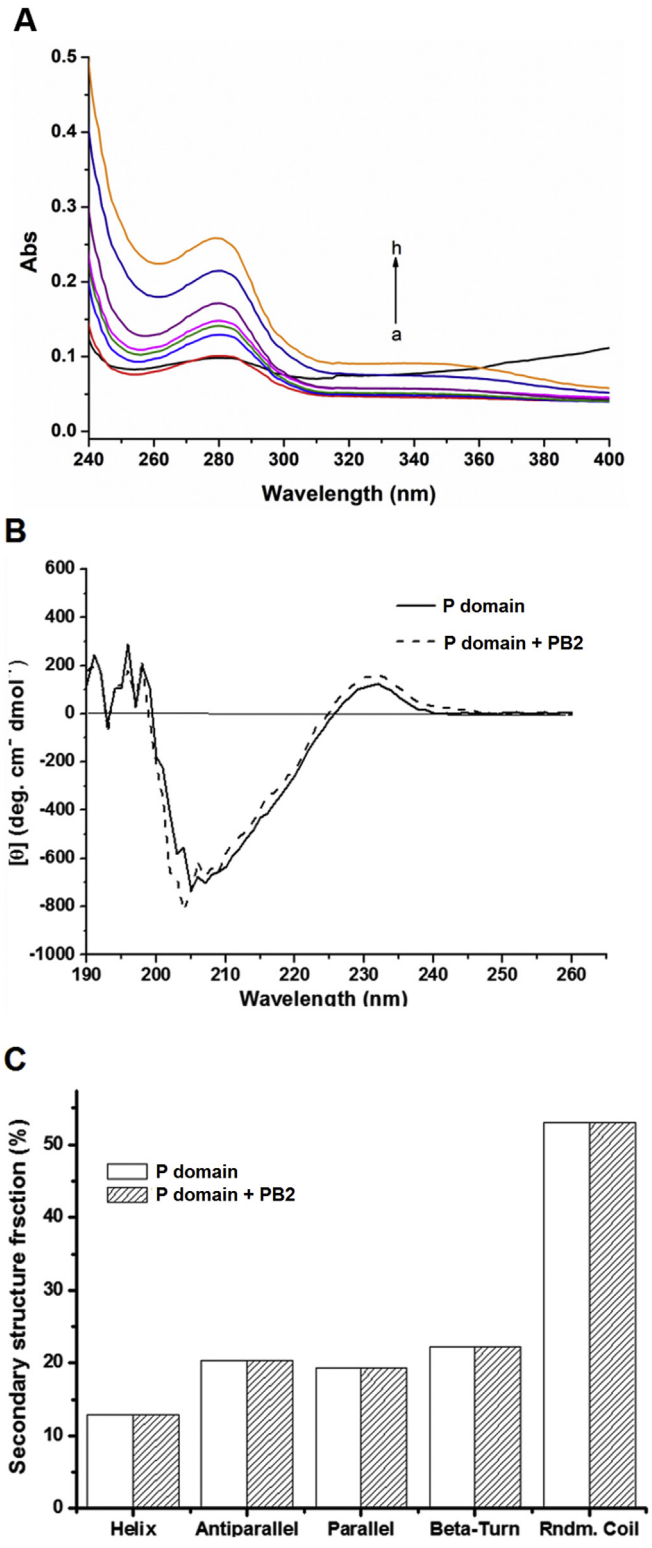


**Fig. 5.** (A) The ultraviolet–visible spectroscopy of P domain (8.41 μM) with PB2 at different concentrations (a, 0 μM; b, 8.41 μM; c, 16.82 μM; d, 24.23 μM; e, 33.64 μM; f, 42.05 μM; g, 50.46 μM; h, 58.87 μM)[PBS] = 10 mM, pH 7.4, 25 °C. (B) CD spectra of P domain with or without PB2. (C) Estimated secondary structural fractions of P domain with or without PB2 by K2D software. Conditions: [P domain] = 8.41 μM in buffer containing 10 mM PBS (pH 7.4), [PB2] = 0.1 mM, 25 °C.

occurred. Capsid proteins that were aggregated by PB2 further confirmed the results above, leading to a speculation that PB2 can change the conformation or block the antigenic binding site of the P domain, to exert an anti-norovirus effect. Our findings are also consistent with the results from Lipson et al. (2012), where the anti-rotavirus activity of procyanidins was determined to be due to a blockage of viral antigenic binding determinants by procyanidins (Lipson et al., 2012).

In summary, using FCV-F9 and MNV-1 as cultivable HNoV surrogates together with studies with VLPs (for HNoV GII.4) and the corresponding P domain, PB2 was found to be capable of decreasing HNoV surrogate titers. PB2 could also bind to the capsid structure as well as to the VLPs and the P domain and caused aggregation of the viral particles. Therefore, the proposed mechanism can only be speculated based on these studies that could potentially be associated with a direct binding between PB2 and viral capsid proteins that cause aggregation of viral particles, change in the viral capsid structure and/or blocking of the antigenic binding sites. Overall, dimeric and polymeric polyphenols show potential as antiviral therapeutic options to prevent HNoV illness.

## Contributions

D. Liu (China) did all the spectra experiments. Dr. J. Deng (China) performed and wrote the part of the biochemical experiments. Dr. S. Joshi (UTIA, USA) did the work on the antiviral activity determination and writing of the section, which was submitted as part of her Ph.D. dissertation (partially supported by the UT Yates Dissertation Fellowship) in partial fulfillment of the requirements for her doctoral degree at UT Knoxville. Dr. P. Liu (Emory, USA) prepared the P-domain and VLPs and edited the manuscript. C. Zhang (China) did the TEM analysis. Y. Yu, R. Zhang and D. Fan (all in China) helped to calculate the spectra parameters. Dr. H. Yang (China) was responsible for designing the interaction mechanism experiments, and writing and editing the manuscript. Dr. D'Souza (UTIA, USA) designed the antiviral study, interpreted the antiviral data, performed analysis and assisted in writing, editing and compiling the manuscript.

## Acknowledgements

This project was supported by the National Natural Science Foundation of China (21306146 and 21676212) and the UT Institute of Agriculture and the Multistate Project S-1056.

## Appendix A. Supplementary data

Supplementary data related to this article can be found at http://dx.doi.org/10.1016/j.fm.2018.06.009.

## References

Alvarez, E., Rodino-Janeiro, B.K., Jerez, M., Ucieda-Somoza, R., Nunez, M.J., Gonzalez-Juanatey, J.R., 2012. Procyanidins from grape pomace are suitable inhibitors of human endothelial NADPH oxidase. J. Cell. Biochem. 113, 1386–1396.

Bartolome, B., Estrella, I., Hernandez, M.T., 2000. Interaction of low molecular weight phenolics with proteins (BSA). J. Food Sci. 65, 617–621.

Brogan, A.P., Widger, W.R., Kohn, H., 2003. Bicyclomycin fluorescent probes: synthesis and biochemical, biophysical, and biological properties. J. Org. Chem. 68, 5575–5587.

D'Souza, D.H., 2014. Phytocompounds for the control of human enteric viruses. Curr. Opin. Virol. 4, 44–49.

D'Souza, D.H., Dice, L., Davidson, P.M., 2016. Aqueous extracts of Hibiscus sabdariffa calyces to control aichivirus. Food Environ. Virol. 8, 112–119.

Ettayebi, K., Crawford, S.E., Murakami, K., Broughman, J.R., Karandikar, U., Tenge, V.R., Neill, F.H., Blutt, S.E., Zeng, X.L., Qu, L., Kou, B., Opekun, A.R., Burrin, D., Graham, D.Y., Ramani, S., Atmar, R.L., Estes, M.K., 2016. Replication of human noroviruses in stem cell-derived human enteroids. Science 353, 1387–1393.

Fino, V.R., Kniel, K.E., 2008. UV light inactivation of hepatitis A virus, aichi virus, and feline calicivirus on strawberries, green onions, and lettuce. J. Food Protect. 71, 908–913.

Gescher, K., Kuhn, J., Lorentzen, E., Hafezi, W., Derksen, A., Deters, A., Hensel, A., 2011. Proanthocyanidin-enriched extract from MyrothamnusflabellifoliaWelw. exerts antiviral activity against herpes simplex virus type 1 by inhibition of viral adsorption and

penetration. J. Ethnopharmacol. 134, 468–474.
Hall, A.J., Lopman, B.A., Payne, D.C., Patel, M.M., Gastanaduy, P.A., Vinje, J., Parashar, U.D., 2013. Norovirus disease in the United States. Emerg. Infect. Dis. 19, 1198–1205.
Hammerstone, J.F., Lazarus, S.A., Schmitz, H.H., 2000. Procyanidin content and variation in some commonly consumed foods. J. Nutr. 130, 2086s–2092s.
Howell, A.B., Reed, J.D., Krueger, C.G., Winterbottom, R., Cunningham, D.G., Leahy, M., 2005. A-type cranberry proanthocyanidins and uropathogenic bacterial anti-adhesion activity. Phytochemistry 66, 2281–2291.
Howell, A.B., Vorsa, N., Der Marderosian, A., Foo, L.Y., 1998. Inhibition of the adherence of P-fimbriated Escherichia coli to uroepithelial-cell surfaces by proanthocyanidin extracts from cranberries. N. Engl. J. Med. 339, 1085–1086.
Jiang, X., Huang, P., Zhong, W., Tan, M., Farkas, T., Morrow, A.L., Newburg, D.S., Ruiz-Palacios, G.M., Pickering, L.K., 2004. Human milk contains elements that block binding of noroviruses to human histo-blood group antigens in saliva. J. Infect. Dis. 190, 1850–1859.
Jiang, X., Wang, M., Graham, D.Y., Estes, M.K., 1992. Expression, self-assembly, and antigenicity of the norwalkvirus capsid protein. J. Virol. 66, 6527–6532.
Joshi, S., Howell, A.B., D'Souza, D.H., 2017. Blueberry proanthocyanidins against human norovirus surrogates in model foods and under simulated gastric conditions. Food Microbiol. 63, 263–267.
Joshi, S.S., Howell, A.B., D'Souza, D.H., 2016. Reduction of enteric viruses by blueberry juice and blueberry proanthocyanidins. Food Environ. Virol. 8, 235–243.
Kageyama, T., Shinohara, M., Uchida, K., Fukushi, S., Hoshino, F.B., Kojima, S., Takai, R., Oka, T., Takeda, N., Katayama, K., 2004. Coexistence of multiple genotypes, including newly identified genotypes, in outbreaks of gastroenteritis due to norovirus in Japan. J. Clin. Microbiol. 42, 2988–2995.
Khurana, S., Venkataraman, K., Hollingsworth, A., Piche, M., Tai, T.C., 2013. Polyphenols: benefits to the cardiovascular system in health and in aging. Nutrients 5, 3779–3827.
Kimmel, E.M., Jerome, M., Holderness, J., Snyder, D., Kemoli, S., Jutila, M.A., Hedges, J.F., 2011. Oligomeric procyanidins stimulate innate antiviral immunity in dengue virus infected human PBMCs. Antivir. Res. 90, 80–86.
Lipson, S.M., Ozen, F.S., Karthikeyan, L., Gordon, R.E., 2012. Effect of pH on anti-rotavirus activity by comestible juices and proanthocyanidins in a cell-free assay system. Food Environ. Virol. 4, 168–178.
Liu, X., Liu, P., Wang, J., Moe, C., Hu, S., Cheng, L., Gu, W., Wang, X., 2015. Seroepidemiology of norovirus GII.3 and GII.4 infections in children with diarrhea in Xi'an, China. Foodb. Pathog. Dis. 12, 500–505.
Lizarraga, D., Lozano, C., Briede, J.J., van Delft, J.H., Tourino, S., Centelles, J.J., Torres, J.L., Cascante, M., 2007. The importance of polymerization and galloylation for the antiproliferative properties of procyanidin-rich natural extracts. FEBS J. 274, 4802–4811.
Mai, H., Jin, M., Guo, X., Liu, J., Liu, N., Cong, X., Gao, Y., Wei, L., 2013. Clinical and epidemiologic characteristics of norovirus GII.4 Sydney during winter 2012-13 in Beijing, China following its global emergence. PLoS One 8, e71483.
Shahat, A.A., Ismail, S.I., Hammouda, F.M., Azzam, S.A., Lemiere, G., De Bruyne, T., De Swaef, S., Pieters, L., Vlietinck, A., 1998. Anti-HIV activity of flavonoids and proanthocyanidins from Crataegussinaica. Phytomedicine 5, 133–136.
Soares, S., Mateus, N., Freitas, V., 2007. Interaction of different polyphenols with bovine serum albumin (BSA) and human salivary alpha-amylase (HSA) by fluorescence quenching. J. Agric. Food Chem. 55, 6726–6735.
Su, X., D'Souza, D.H., 2011. Grape seed extract for control of human enteric viruses. Appl. Environ. Microbiol. 77, 3982–3987.
Su, X., D'Souza, D.H., 2012. Inactivation of human norovirus surrogates by benzalkonium chloride, potassium peroxymonosulfate, tannic acid, and gallic acid. Foodb. Pathog. Dis. 9, 829–834.
Su, X., D'Souza, D.H., 2013. Grape seed extract for foodborne virus reduction on produce. Food Microbiol. 34, 1–6.
Su, X., Howell, A.B., D'Souza, D.H., 2010a. Antiviral effects of cranberry juice and cranberry proanthocyanidins on foodborne viral surrogates–a time dependence study in vitro. Food Microbiol. 27, 985–991.
Su, X., Howell, A.B., D'Souza, D.H., 2010b. The effect of cranberry juice and cranberry proanthocyanidins on the infectivity of human enteric viral surrogates. Food Microbiol. 27, 535–540.
Su, X., Sangster, M.Y., D'Souza, D.H., 2010c. In vitro effects of pomegranate juice and pomegranate polyphenols on foodborne viral surrogates. Foodb. Pathog. Dis. 7, 1473–1479.
Takeshita, M., Ishida, Y., Akamatsu, E., Ohmori, Y., Sudoh, M., Uto, H., Tsubouchi, H., Kataoka, H., 2009. Proanthocyanidin from blueberry leaves suppresses expression of subgenomic hepatitis C virus RNA. J. Biol. Chem. 284, 21165–21176.
Tan, M., Hegde, R.S., Jiang, X., 2004. The P domain of norovirus capsid protein forms dimer and binds to histo-blood group antigen receptors. J. Virol. 78, 6233–6242.
Tan, M., Jiang, X., 2011. Norovirus-host interaction: multi-selections by human histo-blood group antigens. Trends Microbiol. 19, 382–388.
Terra, X., Montagut, G., Bustos, M., Llopiz, N., Ardevol, A., Blade, C., Fernandez-Larrea, J., Pujadas, G., Salvado, J., Arola, L., Blay, M., 2009. Grape-seed procyanidins prevent low-grade inflammation by modulating cytokine expression in rats fed a high-fat diet. J. Nutr. Biochem. 20, 210–218.
Vega, E., Barclay, L., Gregoricus, N., Shirley, S.H., Lee, D., Vinje, J., 2014. Genotypic and epidemiologic trends of norovirus outbreaks in the United States, 2009 to 2013. J. Clin. Microbiol. 52, 147–155.
Xue, L., Wu, Q., Dong, R., Kou, X., Li, Y., Zhang, J., Guo, W., 2013. Genetic analysis of noroviruses associated with sporadic gastroenteritis during winter in Guangzhou, China. Foodb. Pathog. Dis. 10, 888–895.
Yang, H., Liu, Q., Zhao, L., Yuan, Y., Fan, D., Deng, J., Zhang, R., 2014a. Fluorescence spectroscopic studies on the interaction of oleanolicacid and its triterpenoid saponins derivatives with two serum albumins. J. Solut. Chem. 43, 774–786.
Yang, H., Xiao, L., Yuan, Y., Luo, X., Jiang, M., Ni, J., Wang, N., 2014b. Procyanidin B2 inhibits NLRP3 inflammasome activation in human vascular endothelial cells. Biochem. Pharmacol. 92, 599–606.
Yang, Z.F., Bai, L.P., Huang, W.B., Li, X.Z., Zhao, S.S., Zhong, N.S., Jiang, Z.H., 2014c. Comparison of in vitro antiviral activity of tea polyphenols against influenza A and B viruses and structure-activity relationship analysis. Fitoterapia 93, 47–53.
Zhang, X.F., Dai, Y.C., Zhong, W., Tan, M., Lv, Z.P., Zhou, Y.C., Jiang, X., 2012. Tannic acid inhibited norovirus binding to HBGA receptors, a study of 50 Chinese medicinal herbs. Bioorg. Med. Chem. 20, 1616–1623.
Zheng, D.P., Widdowson, M.A., Glass, R.I., Vinjé, J., 2010. Molecular epidemiology of genogroup II-genotype 4 noroviruses in the United States between 1994 and 2006. J. Clin. Microbiol. 48, 168–177.
Zhuang, M., Jiang, H., Suzuki, Y., Li, X., Xiao, P., Tanaka, T., Ling, H., Yang, B., Saitoh, H., Zhang, L., Qin, C., Sugamura, K., Hattori, T., 2009. Procyanidins and butanol extract of Cinnamomi Cortex inhibit SARS-CoV infection. Antivir. Res. 82, 73–81.

## Abbreviations

*HNoVs:* Human noroviruses
*VLPs:* Virus-like particles
*HBGAs:* Human histo-blood group antigens
*HCV:* Hepatitis C virus
*HSV-1:* Simplex virus type-1
*PB2:* Procyanidin B2
*TEM:* Transmission electron microscopy
*CRFK:* Crandell Reese Feline Kidney
*DMEM-F12:* Dulbecco's Modified Eagle's Medium/Ham's F-12
*FBS:* Fetal bovine serum
*PBS:* Phosphate buffered saline
*UV:* Ultraviolet–Visible
*CD:* Circular dichroism
*PCR:* Polymerase chain reaction
*Trp:* Tryptophan
*CJ:* Cranberry juice
*C-PAC:* Cranberry procyanidin
*B-PAC:* Blueberry procyanidin
*BSA:* Bovine serum albumin